

Surface effects of vertically propagating gravity waves in a stratified fluid

By ERLAND KÄLLÉN

Department of Meteorology, University of Stockholm, Arrhenius Laboratory,
S-106 91 Stockholm, Sweden

(Received 7 March 1986 and in revised form 19 September 1986)

A linear, stationary internal-wave model is used to determine the vertical propagation of gravity waves produced by submerged moving bodies in a stratified fluid. The turbulent wake generated by the moving object is taken into account parameterically. If the stability of the stratification above the body increases (i.e. the body is under a thermocline) resonance effects occur. Large-amplitude internal waves are generated and they give rise to strong divergence fields at the water surface. These will persist far downstream of the object and are potentially detectable. Limitations of the linear model and comparisons with experimental results available in the literature are discussed.

1. Introduction

A moving underwater object will create a field of internal waves. These waves will propagate upwards and leave some trace on the water surface. In this paper we attempt to study this internal wave field with a steady, linear model and we are mainly interested in the surface effects.

Surface effects from internal waves have been found in several studies using satellite radar (Apel & Gonzales 1983; Alpers & Hennings 1984, and others) and these wave fields are usually associated with distinct features of the bottom topography. Tidal currents of about 1 m s^{-1} over sandbanks in the North Sea produce clearly visible wave trains at the surface (Alpers & Hennings 1984). The surface waves, as seen by radar imagery, reflect the amplitude of the capillary waves which are always present on the water surface. The amplitude of the capillary waves is assumed to be modulated by the divergence/convergence produced by the internal waves. This divergence is typically of the order 10^{-4} to 10^{-3} s^{-1} (Alpers & Hennings 1984).

Our main interest is thus to see whether the internal wave produced by a moving underwater object is sufficiently strong to produce a surface divergence field of about 10^{-3} s^{-1} . We also want to investigate the spatial structure of the divergence field and its sensitivity to the stratification in the ocean. In particular we are interested in the effect of a strong thermocline. We shall assume that the wave field of a moving object is stationary relative to a coordinate system moving with the speed of the body. Furthermore, we assume that the basic stratification is unaffected by the internal wave field and thus we can study the waves using linear theory.

The internal waves in our model are generated by a prescription of a vertical velocity field in a horizontal plane, which forms the lower boundary (figure 1). The vertical velocity field can be calculated when the form of the body and the basic flow speed is known. From experimental studies (Lin & Pao 1979), we know that a moving submerged body will create a turbulent wake and this wake will also give rise to

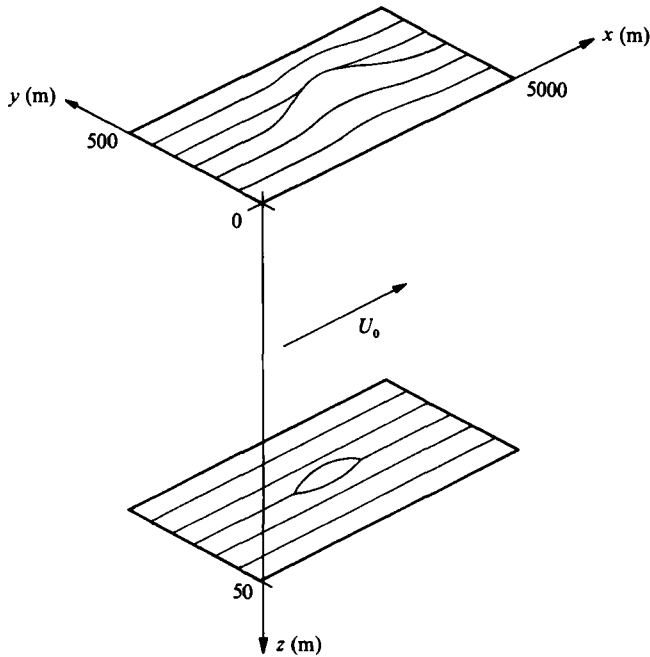


FIGURE 1. The three-dimensional structure of the model used in the present study.

internal waves. Our model is not capable of describing the formation of a wake, but if we assume the form of the wake to be known we can estimate the internal wave field that is created.

In a combined experimental and theoretical study Gilreath & Brandt (1985) show how well a linear model reproduces the results from water-tank experiments. Their linear model does very well in reproducing the body-generated internal wave field, is less skillful in describing the turbulent-wake-produced waves and is not at all good in describing effects due to propeller swirl. In this study we shall concentrate on the wake-generated wave and use a more general form of the lower boundary condition to take into account the wake structure. We thus hope to obtain a better description of the wake-generated disturbance.

We shall assume the wake to be an extension of the body with a form given by the experimental data of Lin & Pao (1979). The lengthscale of the wake is such that the frequency of the internal waves produced is close to the Brunt-Väisälä frequency of the basic stratification. We thus expect the waves generated by the wake to be near resonance and thus to give rise to high-amplitude responses.

The model together with the boundary conditions will be described in §2. In §3 model results will be displayed. First some simple analytical solutions will be presented and then numerical simulations with realistic basic states and a detailed prescription of the lower boundary condition are shown. Two basic states are discussed, one winter situation with no thermocline and one late summer or autumn situation with a strongly developed thermocline. Finally some conclusions are drawn regarding the applicability of the model results.

2. The model

The model to be used in this investigation is a linearized, stationary wave model based on the Boussinesq approximated equations of motion. We thus assume a coordinate system that is stationary relative to the moving object and our lower boundary condition will be that the fluid particles follow the surface of the moving body and its associated wake. By assuming stationarity we do not describe transient wave phenomena, but according to the study of Sharman & Wurtele (1983) this restriction is not very serious. They compared results from a linear stationary lee-wave model with equilibrium flow patterns from time integrations with a fully nonlinear, primitive-equations model and they could see no significant differences. When we investigate the wake that forms behind the body, we shall simply assume the wake to be an extension of the moving body for the purpose of the lower boundary condition. The upper boundary condition is that there are no horizontal pressure differences along the water surface.

Following Smith (1980), who studied internal gravity waves generated by small-scale topography, we may write our linearized stationary model as follows:

$$\left. \begin{aligned} \rho_0(U_0 u_x + U_{0z} w) &= -p_x, \\ \rho_0 U_0 v_x &= -p_y, \\ \rho_0 \left(U_0 w_x - \frac{\rho}{\rho_0} g \right) &= -p_z, \\ u_x + v_y + w_z &= 0, \\ U_0 \rho_x + \rho_{0z} w &= 0. \end{aligned} \right\} \quad (1)$$

The velocities in the x -, y - and z -directions are given by $U_0(z) + u$, v and w respectively where lower case letters indicate perturbation quantities. The pressure perturbation is given by $p_0(z) + p$ and the density variations are described by $\rho_0(z) + \rho$, where p and ρ are perturbation quantities. The basic state is defined by $U_0(z)$ and $\rho_0(z)$. The acceleration due to gravity, g , appears in the Boussinesq approximated buoyancy term in the vertical equation of motion. Note that $g > 0$, and the sign of the buoyancy term in (1) is due to our choice of direction of the vertical coordinate axis, z .

The basic-state density is given by the temperature, salinity and depth below the water surface of the undisturbed fluid. As we wish to determine the response of the model under different temperature and density stratifications, we use the equation of state for sea water given by Fofonoff (1962), which reads

$$\rho_0 = \left(\frac{\lambda(T, S)}{p_0(z) + p_{00}(T, S)} + \alpha_0 \right)^{-1},$$

where T is the temperature in $^{\circ}\text{C}$ and S is the salinity in parts per thousand. Also compressibility effects on the density are taken into account through the inclusion of the term $p_0(z)$. These effects are, however, very small for the depth intervals of interest to us. The constants λ , p_{00} and α_0 are obtained from Fofonoff (1962).

The linear system of partial differential equations defined by (1) are solved through a separation of variables. In the horizontal plane we make a Fourier decomposition

of the perturbation quantities and are thus able to reduce the system to an ordinary differential equation in the vertical direction. We write

$$\begin{pmatrix} u \\ v \\ w \\ \rho \\ p \end{pmatrix} = \sum_{j_1, j_2}^N \sum_{\substack{k=(2\pi/L_x)j_1 \\ l=(2\pi/L_y)j_2}} \begin{pmatrix} \hat{u}_{kl} \\ \hat{v}_{kl} \\ \hat{w}_{kl} \\ \hat{\rho}_{kl} \\ \hat{p}_{kl} \end{pmatrix} e^{i(kx+ly)},$$

where L_x and L_y are the maximum lengthscales in the x - and y -directions respectively. We thus assume the wave field to be periodic outside this domain. By inserting the spectral expansion into (1) we obtain for each combination of k and l

$$\left. \begin{aligned} \rho_0(ikU_0 \hat{u} + U_{0z} \hat{w}) &= -ik\hat{p}, \\ \rho_0 ikU_0 \hat{v} &= -il\hat{p}, \\ \rho_0 ikU_0 \hat{w} - g\hat{\rho} &= -\hat{p}_z \\ ik\hat{u} + il\hat{v} + \hat{w}_z &= 0, \\ ikU_0 \hat{\rho} + \rho_{0z} \hat{w} &= 0. \end{aligned} \right\} \quad (2)$$

By eliminating \hat{u} , \hat{v} , $\hat{\rho}$ and \hat{p} in this linear system of equations we finally obtain

$$\hat{w}_{zz} + A(z) \hat{w}_z - B(z) \hat{w} = 0, \quad (3a)$$

where
$$A(z) = \frac{\rho_{0z}}{\rho_0}, \quad (3b)$$

$$B(z) = (k^2 + l^2) \left(1 - \frac{g\rho_{0z}/\rho_0}{k^2 U_0^2} + \frac{1}{\rho_0} \frac{d}{dz} (\rho_0 U_{0z}) \right). \quad (3c)$$

Equation (3) is our governing second-order differential equation for the internal wave field.

Supplemented with proper boundary conditions it can be solved for each pair of wavenumbers (k, l) separately. The total solution may then be found through linear superposition.

2.1. Boundary conditions

Our two boundary conditions are at the upper surface and the depth of the moving body. We start by considering the upper surface where we assume the pressure perturbation to be zero. This implies that along the surface, where we define $z = \zeta$, we have a constant atmospheric pressure p_0 . Using the hydrostatic equation for water this boundary condition may be linearized around $z = 0$ and written

$$p_{z=0} = p_0 - \rho_0 g \zeta. \quad (4)$$

The linearization also implies that we can write the upper-surface displacement ζ as

$$\zeta = \frac{1}{U_0} \int_0^x w_{z=0} dx. \quad (5)$$

As we wish to apply our equations using the variable w we must rewrite our upper

boundary condition in terms of w . The horizontal equations of motion at the upper boundary may be written

$$\left. \begin{aligned} U_0 u_x + U_{0z} w &= g\zeta_x, \\ U_0 v_x &= g\zeta_y, \end{aligned} \right\} \quad (6)$$

where we have used (4) to write the pressure gradient in terms of ζ .

Together with the continuity equation

$$u_x + v_y + w_z = 0 \quad (7)$$

we may eliminate u and v from (6) and (7) to obtain

$$-U_0 w_{xz} + U_{0z} w_z - g\nabla^2 \zeta = 0. \quad (8)$$

By using (5) and the Fourier transform of w we find our upper boundary condition in terms of \hat{w} to be

$$U_0^2 k^2 \hat{w}_z - (U_{0z} U_0 k^2 - g(k^2 + l^2)) \hat{w} = 0. \quad (9)$$

A scale analysis of this equation (Phillips 1966) shows that the second term in (9) dominates strongly over the first and therefore the upper boundary condition may be simplified to read

$$\hat{w} = 0 \quad (10)$$

to a very good approximation. This implies an absence of any surface wave field but we may still have surface divergence/convergence effects as we have not assumed \hat{w}_z to be zero. In our numerical experiments we shall use the surface boundary condition in the form given by (9) as this does not introduce any computational difficulties and we are still interested in surface displacements although they may be very small.

At the lower boundary ($z = H$) we assume the fluid particles to follow the surface of the object and its associated wake. Denoting the surface of the body/wake by $z = H - h(x, y)$ this boundary condition can be written

$$(U_0 + u, v) \cdot \nabla h + w = 0. \quad (11)$$

In a linearized form the boundary condition becomes

$$w(H) = -U_0(H) \frac{\partial h}{\partial x}. \quad (12)$$

The linearization assumes $h \ll H$ and also $\partial h / \partial x$ to be small. If $\partial h / \partial x$ is of order unity the perturbation velocity w is of the same size as the basic current speed U_0 and then our linear model breaks down. In the problem that we attempt to study there are situations where $\partial h / \partial x$ may be very large, i.e. on the forward edges of the turbulent wake which is assumed to have a parabolic shape.

In a previous study (Gilreath & Brandt 1985) the shape of the body was assumed to be in the form of a Rankine ovoid. By assuming a potential flow around such a body an explicit form of the vertical velocity field can be found. The potential-flow assumption is reasonable owing to the large Froude number (normally of the order 10^2). With this boundary condition singular points in the vertical velocity field are avoided, but the body and wake are restricted to ellipsoidal shapes with variable aspect ratios. Here, we want to specify a more general shape of the body and we thus wish to obtain the vertical velocity from an arbitrary body shape according to (12). We shall, however, avoid singularities at stagnation points by artificially smoothing the body shape close to such points. In §3.2 we shall show explicitly how such a smoothing is done.

2.2. Wake structure

A self-propelled moving underwater object will create a turbulent wake. The wake will form behind the body and it will expand in time, both horizontally and vertically. Through simple dimensional arguments (Landau & Lifshitz 1959) it may be deduced that the wake has a parabolic shape in its initial stage of development. In a neutrally buoyant fluid the parabolic shape will be found even at long distances behind the body, but if the fluid is stratified the wake will collapse vertically. This wake collapse appears at a certain distance downstream of the moving body and it will produce a significant internal wave field which propagates horizontally and vertically. The numerical modelling of such a wake collapse is difficult; some attempts have been reported in the literature (Hassid 1980) but in general it requires a large amount of computer capacity. Such a model is outside the scope of this investigation; we are only interested in the internal wave structure produced by the wake and thus only wish to introduce the wake as a boundary condition in our internal wave model.

Experimental investigations of the wake structure in a stratified fluid have shown that the wake collapse is governed by the basic flow parameters, namely the flow speed and the Brunt-Väisälä frequency. In a review paper Lin & Pao (1979) have demonstrated that the wake collapse occurs at a distance of $0.23 U_0/N$ from the wake onset, where N is the Brunt-Väisälä frequency of the vertical stratification. This relation gives a good description of the experimental results if the Froude number is above 60. The Froude number is then defined as $F = U_0/ND$, where D is the diameter of the cross-section of the body. In the ocean and for a body with a diameter of 10 m, F is typically around 100. We shall thus make extensive use of the experimental results of Lin & Pao (1979) in specifying the wake dimensions.

We shall assume that at the wake onset the shape of the wake is parabolic (see figure 2). After the critical distance of $0.23 U_0/N$ we assume a wake collapse in the vertical direction, and a slight wake spreading in the horizontal plane. In a vertical plane perpendicular to the direction of motion we shall assume that the wake initially has a cylindrical cross-section. After the wake collapse, the cross-section is elliptical. The maximum wake height is taken to be $0.55DF_b^{\frac{1}{2}}$, in agreement with the experimental results of Lin & Pao (1979).

The structure of the wake is sketched in figure 2, and with typical parameter values inserted ($N \sim 10^{-2} \text{ s}^{-1}$, $U_0 \sim 5 \text{ m s}^{-1}$) we obtain a typical horizontal lengthscale of the wake of 500 m. The maximum height of the wake is found to be $\frac{3}{4}D$. This is a reasonable number for a linear lower boundary condition to be valid. We see, however, that the wake lengthscale is an order of magnitude larger than the typical lengthscale of the body. We thus expect the internal waves produced by the wake to propagate upwards much more readily than the waves produced by the object itself. This is because the frequency of these waves (typically $U_0/L \sim 10^{-2} \text{ s}^{-1}$) is close to the Brunt-Väisälä frequency of the basic stratification, in particular if we have a marked thermocline. The model is thus close to resonance and we may expect large-amplitude responses to weak forcings.

When we specify only the wake boundaries we implicitly assume that they act as impermeable walls to the surrounding flow. We thus consider the wake as an extension of the solid body. This view of the wake is true to a certain extent; gradients in the mean flow occur at the wake boundaries (Lin & Pao 1979) which implies that part of the flow must go around rather than through the wake. How much of the flow actually goes over the wake and thus creates internal waves is difficult to judge from the experimental data available in the open literature. In our simple model we

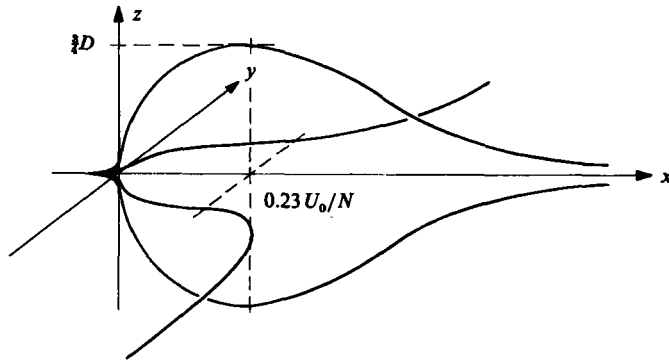


FIGURE 2. The assumed three-dimensional profile of the wake. The maximum height of the body is D , the basic velocity U_0 and the Brunt-Väisälä frequency of the fluid is N .

can only assume that the wake boundaries act as a solid body with a certain efficiency factor α , which is less than one. The bottom boundary condition (11) can then be written

$$(U_0 + u, v) \cdot \nabla(\alpha \hat{h}) + w = 0. \quad (13)$$

The efficiency factor enters the equation as a linear scaling of the wake height. Owing to the linearity of the wave model this scaling factor may equally well be applied to the resulting internal-wave or surface-wave height. For the purpose of judging our results we can see the efficiency factor as a reduction factor by which the results should be multiplied. Owing to our poor knowledge of α we have not included it in the computations and the numerical results should thus be seen as upper bounds indicating the correct order of magnitude. The problem of exactly how a wake collapse generates internal waves seems to be a subject that is under intensive research (Lin & Pao 1979).

3. Model results

In this section we shall present some model solutions to show the characteristic features of the internal wave field generated by a moving object. We first examine the general properties of the solutions by analytical methods and then show results from numerical simulations with different basic states and boundary conditions.

3.1. Analytical solution

If we assume U_0 and the Brunt-Väisälä frequency $N = [(g/\rho_0)(d\rho_0/dz)]^{1/2}$ to be independent of depth, the vertical-structure equation of the model, (3), may be written

$$\hat{w}_{zz} + \frac{N^2}{g} \hat{w}_z - (k^2 + l^2) \left(1 - \left(\frac{N}{kU_0} \right)^2 \right) \hat{w} = 0. \quad (14)$$

Supplemented with the boundary conditions $w = 0$ at $z = 0$ and $w = ikU_0 \hat{h}$ at $z = H$, where \hat{h} is the Fourier-transformed lower boundary profile, we easily find a solution of the form

$$\hat{w} = C \exp \left[-\frac{N^2}{2g} (z - H) \right] \frac{\sinh(rz)}{\sinh(rH)}, \quad (15)$$

where

$$C = ikU_0 \hat{h}$$

and

$$r = \left[\left(\frac{N^2}{2g} \right)^2 + (k^2 + l^2) \left(1 - \left(\frac{N}{kU_0} \right)^2 \right) \right]^{\frac{1}{2}}.$$

With characteristic parameter values ($N \approx 10^{-2} \text{ s}^{-1}$, $U_0 \approx 5 \text{ m s}^{-1}$, $g \approx 10 \text{ m s}^{-2}$) and a wavelength of 10^2 m ($k = 2\pi \times 10^{-2} \text{ m}^{-1}$) we may make the approximation $r = (k^2 + l^2)^{\frac{1}{2}}$ and our solution is damped only with height. The damping decreases with increasing wavelengths and for $k = N/U_0$ implying a wavelength of around $3 \times 10^3 \text{ m}$, the solution is only weakly damped owing to the factor $\exp[-N/2g(z-H)]$ which implies propagating waves with an e-folding distance of about $2 \times 10^4 \text{ m}$. This should be compared with the e-folding distance of a wave with a wavelength of 10^2 m which is 16 m . Even shorter waves are damped out within a very short distance from the wave generator and thus we do not expect the spikes produced by the linear boundary condition at isolated stagnation points to be of significance for the propagating part of the wave spectrum. On the other hand we see that if N becomes large at some level (thermocline) then an exponentially decaying solution may transform into a propagating solution. This type of behaviour may give rise to large-amplitude responses for some parts of the generated spectrum while other parts are suppressed. We may thus obtain a resonant excitation of an intrinsic frequency and to see more clearly how such a solution behaves we shall now turn to the numerical experiments.

3.2. Numerical results

Our numerical model is written in a spectral form for the horizontally varying part of the solution, while the vertical variation is found through a solution of (3) for each wave component. The total solution is then constructed via a linear superposition of all the wave components. In the general case, where the basic stratification and the basic-state current vary with height, (3) can be solved with a shooting method. We have used here a standard library (IMSL) routine with a specified relative error tolerance of 1%.

The upper boundary condition is given by (9) while the lower boundary condition is given in a linear form, (12), which in spectral space may be written

$$\hat{w} = ikU_0 \hat{h}. \quad (16)$$

To construct the wake profile, we have used the qualitative features described by Lin & Pao (1979). In its initial stage the wake is assumed to be circularly symmetric in a plane perpendicular to the direction of motion and with a parabolic profile in a vertical plane parallel to the x -axis. The wake collapses in the vertical plane at a distance x_c from the body, where x_c is defined as $0.23 U_0/N$ (see the previous discussion of wake structure and figure 2). At the same point the wake is assumed to spread horizontally. In a mathematical form the wake with height $H(x)$ and width $W(x)$ may be described by the equations

$$H(x) = \frac{3}{2}D \frac{(x/x_c)^2}{1 + (x/x_c)^4}, \quad (17a)$$

$$W(x) = \begin{cases} \frac{3}{2}D \frac{(x/x_c)^2}{1 + (x/x_c)^4} & \text{if } x \leq x_c, \\ \frac{3}{4}D \left(\frac{x}{x_c} \right)^{0.4} & \text{if } x > x_c, \end{cases} \quad (17b)$$

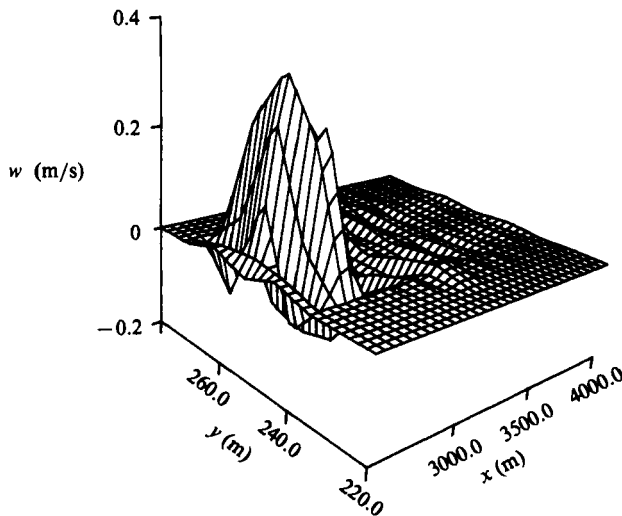


FIGURE 3. Vertical velocity field produced by the wake described by (25) and the linear boundary condition defined by (16).

where D is the diameter of the body and $\frac{3}{4}D$ is, as discussed in §2.2, the empirically determined maximum wake height. This maximum occurs at $x = x_c$. The vertical velocities produced by this wake when the linear boundary condition is applied are shown in figure 3. For this wake profile the maximum amplitude of the vertical velocities occurs at roughly $0.8x_c$ rather than at the stagnation point. In order to achieve this we have specified the forward edge of the wake slightly differently than the measurements of Lin & Pao (1979) would suggest. Instead of $H(x) \sim x^{\frac{1}{2}}$ for small x , we have here given $H(x) \sim x^2$. This choice avoids a singularity in $H'(x)$ at $x = 0$ and thus the problem of large vertical velocities in the linear boundary condition. The motivation for this choice is the close resemblance to potential flow because of the high Froude number. At the onset of the wake the flow is similar to potential flow around a sphere near a stagnation point. The streamlines for such a flow can be approximated with parabolas. We have also performed calculations with a singularity in $H'(x)$, but the results produced are not very different. This is because the short waves produced by the singularity are efficiently damped out by the model. A large-amplitude spike in the vertical velocities will, however, also affect the long waves of the model in an unsatisfactory manner. In order to avoid this problem we have specified the wake in such a way that it produces a smooth vertical velocity profile at the lower boundary.

With this wake profile we show results from two numerical experiments which differ in their specification of the density stratification above the wake. In both cases we have a weak stratification at the depth of the object (50 m) which gives us a local Froude number of 37 for a body diameter D of 14 m. In experiment I the stratification is unchanged throughout the depth of the fluid and a cross-section of the resulting wave field is shown in figure 4. A basic feature of the wave field is a rapid decrease of the amplitude and a spreading of the wave as it propagates upward. In figures 5 and 6 we see the horizontal structure of the wave field at 25 m depth and at the surface. The spreading of the wave is very marked. At 25 m depth we observe a characteristic V-shaped lee-wave pattern which also can be found in the experimental results of Gilreath & Brandt (1985). At the surface we see an amplitude of only 3 cm,

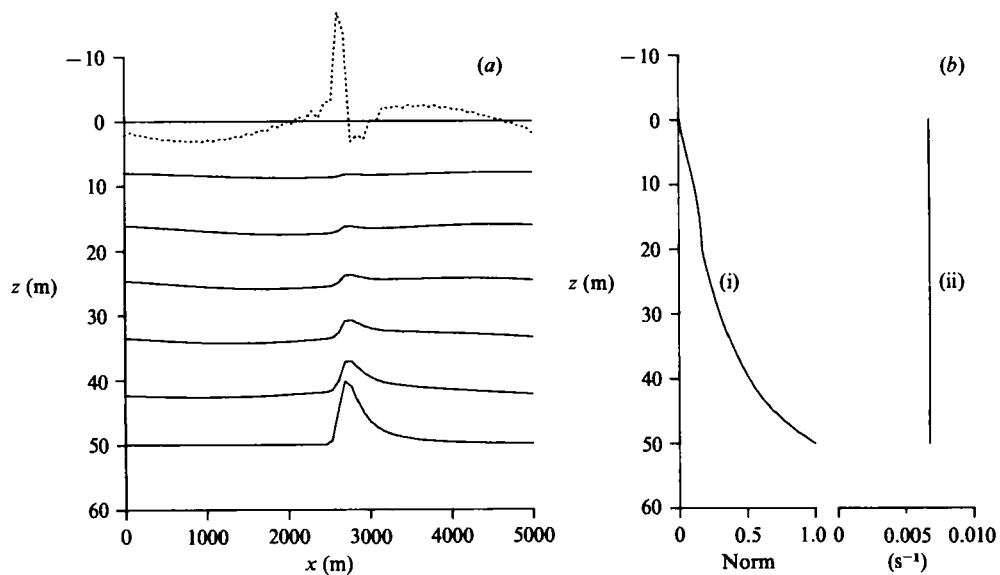


FIGURE 4. (a) Cross-section of the internal wave field created by the vertical velocity field given in figure 3. Also shown (b) is the maximum wave amplitude (i) (relative units) and the Brunt-Väisälä frequency (ii) of the basic stratification as a function of depth. The dotted line gives the horizontal structure of the divergence field at the surface. Maximum divergence amplitude is $3 \times 10^{-3} \text{ s}^{-1}$. Parameter values are: $U_0 = 5 \text{ m s}^{-1}$; $\frac{3}{4}D = 10 \text{ m}$; maximum length in x -direction 5000 m; maximum length in y -direction 500 m; horizontal wavenumber truncation 64 (same in both directions); number of gridpoints in the vertical 31.

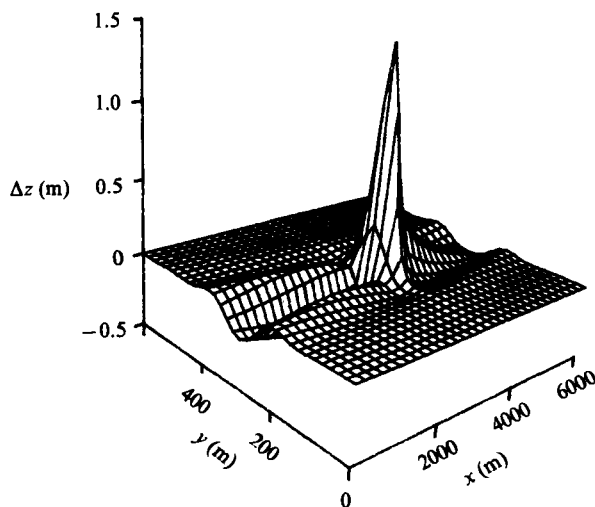


FIGURE 5. Horizontal structure of internal wave at $z = 25 \text{ m}$ for experiment I.

which is consistent with the scaling of the boundary condition discussed in §2.1. Instead we have a fairly strong divergence field at the surface, and the structure of the divergence field in the x -direction is shown by the dotted line in figure 4. The maximum amplitude is about $3 \times 10^{-3} \text{ s}^{-1}$ which, according to Alpers & Hennings (1984), is sufficient to cause a significant modulation of the capillary waves on the water surface. There is a marked difference in the horizontal lengthscales of the

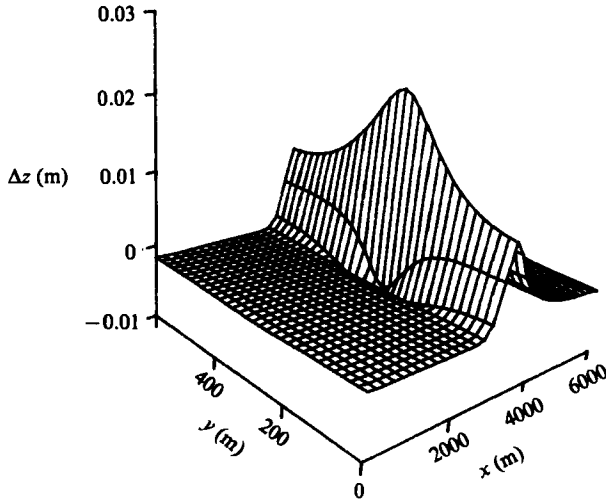


FIGURE 6. Horizontal structure of surface wave in experiment I.

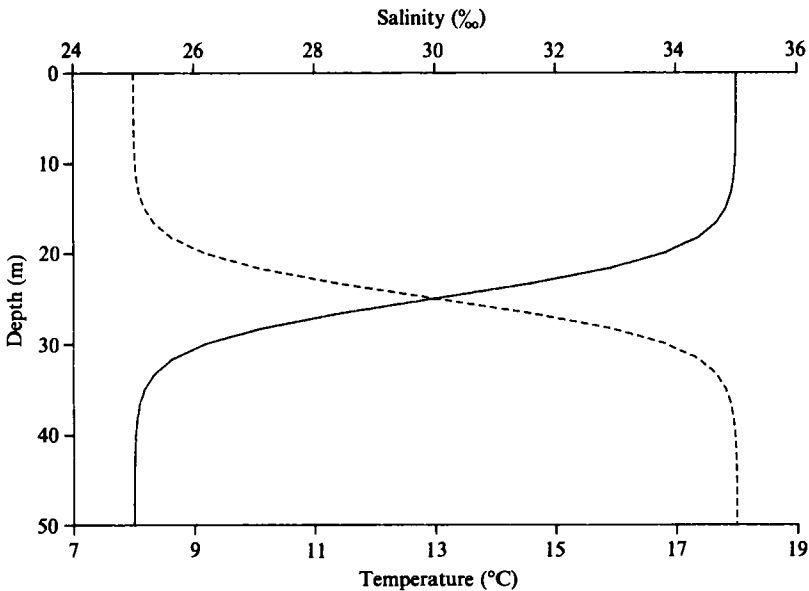


FIGURE 7. Basic stratification of salinity (dashed curve) and temperature (full line) in experiment II.

surface divergence field and the surface wave field. The divergence field is much more concentrated and has almost the same horizontal extent as the wake, while the surface wave has a much broader structure. Despite its low amplitude the surface wave could thus be detectable at longer distances from the moving object than the surface divergence field.

In experiment II a stratification with a very sharp thermocline at 25 m depth is chosen. The temperature and salinity stratifications are given in figure 7 and the resulting density profile is given in figure 8 in terms of the Brunt-Väisälä frequency. Figure 8 also shows a vertical cross-section of the internal wave field. A part of the

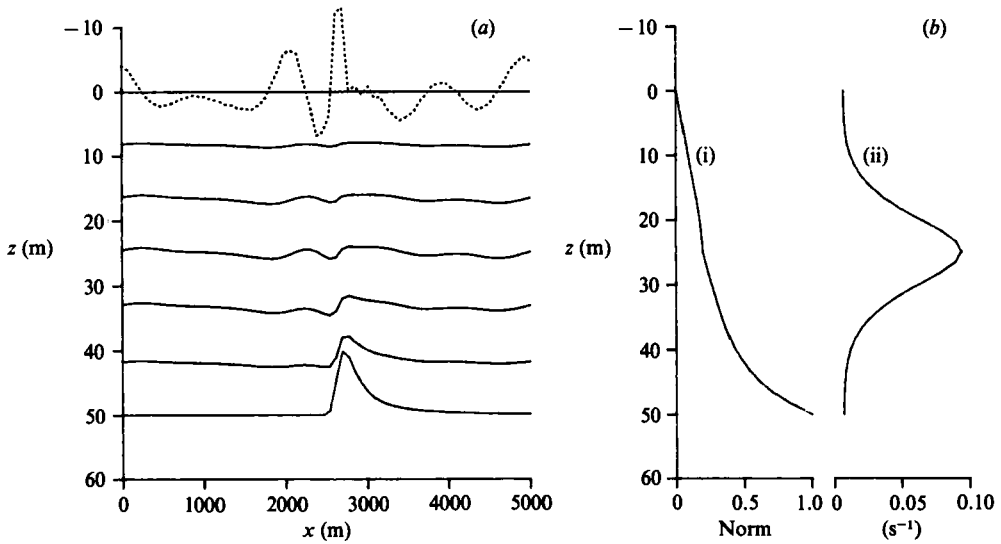


FIGURE 8. Same as figure 4, but for experiment II.

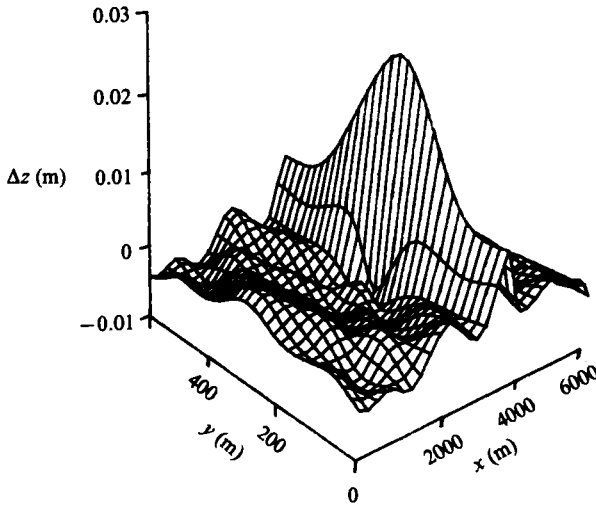


FIGURE 9. Horizontal structure of the surface wave in experiment II.

internal wave field is now of the freely propagating type and we see a very marked resonant response for a wavelength of about 700 m. With an object speed of 5 ms^{-1} this corresponds to a frequency of 0.05 s^{-1} which agrees well with the average Brunt-Väisälä frequency of the thermocline. The divergence field at the surface is stronger than in case I and it has a much more complicated spatial structure. Part of this spatial structure is due to the periodicity requirement at the domain boundaries, but we clearly see the resonant 'lee wave' in the surface divergence field. This 'lee wave' appears to extend far downstream of the moving object and is a result of the resonance occurring in the thermocline.

The amplitude of the internal wave field decreases to almost zero at the surface, but we see from figures 4 and 8 that the main difference between experiments I and II lies in the flattening of the amplitude response curve of experiment II around the

thermocline. This is also a manifestation of the resonant response at this level. At the thermocline level, the internal wave field has a significant amplitude (about 15% of its original amplitude) and thermocline oscillations should be detectable. The surface wave in experiment II (figure 9) is not very different from the one found in experiment I. The maximum amplitude is the same, about 3 cm, while there is more amplitude in the wave harmonics in case II owing to resonant amplification.

For an object placed inside the thermocline, the present model failed to converge. In this case the local Froude number is very low (around 5) and therefore the wake parameterization described in §2.2 is not applicable. On physical grounds it can be expected that the vertical wake spreading will be inhibited, but on the other hand we may obtain a very marked resonant amplification of the internal wave. This resonant response is the main reason why our linear model did not converge and in order to model this situation accurately a more sophisticated technique has to be used. Lin & Pao (1979) also state that experimental data for low-Froude-number situations is lacking.

4. Conclusions

We have demonstrated here with a linear model the structure of the internal wave field that can be expected to arise due to a moving underwater object. The turbulent wake that forms behind the body is of crucial importance for the generation of vertically propagating internal waves and the specification of this wake is in our study taken from experimental data (Lin & Pao 1979). The horizontal wavelength of the turbulent wake is determined by the speed of the object U_0 and by the Brunt-Väisälä frequency of the basic stratification N at the depth of the object, and it is roughly equal to U_0/N . We thus have a Froude number close to unity for the horizontal lengthscale defined by the turbulent wake.

If the stratification above the object is unchanged, i.e. the Brunt-Väisälä frequency is constant, the wave will propagate upwards while decreasing in amplitude. At the surface there will be a low-amplitude surface wave (a maximum height of order 10^{-2} m) and a divergence field with an amplitude of order 10^{-3} s $^{-1}$. The surface pattern will have a horizontal lengthscale similar to the lengthscale of the wake.

If the stratification above the object is more stable than at the depth of the object, the propagating wave will be markedly different. In particular if we have a strong thermocline there will be a resonant amplification of certain wavelengths which will show up strongly in the surface signature. The divergence field in this case is somewhat stronger, but still of order 10^{-3} s $^{-1}$. The amplitude of the surface wave remains unchanged, around a few cm. In the divergence field we observe a lee-wave pattern which must be due to a resonant excitation of the thermocline. Because of the model limitations, in particular the fixed sidewall, the resonant amplification is overestimated but there are sound physical reasons to believe that this excitation of the thermocline may persist far downstream of the moving object. The internal dissipation mechanism in the ocean is so weak that it will take a very long time for these oscillations to die out (Badulin, Shira & Tsimring 1985).

An estimate of the vertical eddy diffusivity at the surface, which acts to destroy the surface oscillations, can be made from observations. An estimate of the surface-eddy diffusion coefficient was made from the data given by Kullenberg (1977) and Larsson & Rodhe (1979). We obtain a vertical turbulent exchange coefficient K around 2×10^{-3} m 2 s $^{-1}$ (for details of this derivation, see Källén, Johansson & Lundberg 1984). This is much larger than that normally assumed for the internal

turbulent exchange coefficient ($10^{-4} \text{ m}^2 \text{ s}^{-1}$), but since wind-induced turbulence is created at the water surface we still find the value to be reasonable. Defining a dissipation timescale τ as

$$\tau = \left(\frac{K}{w} \frac{\partial^2 w}{\partial z^2} \right)^{-1} \quad (18)$$

we can estimate τ at the surface by using our governing equation (3) to eliminate $(1/w)/(\partial^2 w/\partial z^2) \sim B(0)$. At the surface N is much less than the maximum N which occurs at the thermocline, and it is mainly the maximum N which determines the propagating wavelength. The coefficient B at $z = 0$ may then be approximated as

$$B(0) \approx k^2 + l^2. \quad (19)$$

We thus finally obtain a timescale

$$\tau = (K(k^2 + l^2))^{-1} \approx \frac{1}{Kl^2}, \quad (20)$$

where the last approximation is because the surface pattern has a much shorter lengthscale across the direction of motion than along it. With a typical lengthscale of order 10^2 m we obtain a timescale of order 10^4 s , i.e. few hours. This implies that under favourable conditions, i.e. with a strong thermocline, the surface pattern should be observable for tens of km behind a moving object. An observation of the surface pattern formed in the wake behind a shipwreck situated in a strong current (W. Alpers, personal communication) supports this theoretical result.

In our conclusions we have only indicated orders of magnitude in the response and this is due to the model limitations. We cannot expect our results to be directly applicable to a realistic situation, but we think that the model results indicate under which external conditions we are most likely to find a surface signal from a moving underwater body.

As the model is linear, no nonlinear effects such as solitary waves can be described. From the experimental results of Gilreath & Brandt (1985) it may be concluded that if the thermocline is sufficiently sharp, solitary waves can be excited and these will propagate over long distances with unchanged shape. The excitation of solitary waves will thus enhance the wave signal from the underwater body in addition to the resonant effects described here.

We have also been able to conclude that the signal is strong enough to be detectable by for example radar imagery, but internal sensors in the ocean should also be useful. The largest amplitudes of the internal waves are found in the ocean and by for example registering the height of the thermocline as a function of time an internal-wave signal could be detected. It is then still questionable whether the signal-to-noise ratio is sufficient to allow detection of the signal. Experiments in the open ocean with various types of detection systems are necessary in order to establish whether this is the case. Descriptions of such experiments in the open literature are difficult to find.

In water-tank experiments Gilreath & Brandt (1985) find that their internal-wave registrations are not reproducible aft of a certain distance behind the moving body. This horizontal distance increases as the vertical distance to the body is increased. The irreproducibility of the internal wave field is attributed by Gilreath & Brandt (1985) to intermittent turbulent bursts. These bursts are of course not captured by our linear model but they indicate another mechanism by which internal waves are produced. As the bursts form far downstream of the object they act as additional

wave generators producing signals which may be detectable at the surface. The irreproducibility of the internal wave may thus not prevent the detection of signals related to the moving object. Whether these signals are strong enough in comparison with the background, random internal wave field can only be found through field experiments as noted above.

This study would not have been undertaken without the continuous support and encouragement of Dr Sture Wickerts. I also wish to thank one anonymous reviewer and Dr F. Berkshire for helpful and constructive criticism.

REFERENCES

- ALPERS, W. & HENNINGS, I. 1984 A theory of the imaging mechanism of underwater bottom topography by real and synthetic aperture radar. *J. Geophys. Res.* **89**, 10529–10546.
- APEL, J. & GONZALES, F. 1983 Nonlinear features of internal waves off Baja, California as observed from the SEASAT imaging radar. *J. Geophys. Res.* **88**, 4459–4466.
- BADULIN, S. I., SHRIRA, V. I. & TSIMRING, L. SH. 1985 The trapping and vertical focusing of internal waves in a pycnocline due to the horizontal inhomogeneities of density and currents. *J. Fluid Mech.* **158**, 199–218.
- FOFONOFF, N. P. 1962 Physical properties of sea-water. In *The Sea*, vol. I (ed. M. N. Hill), pp. 3–28. Wiley.
- GILREATH, H. E. & BRANDT, A. 1985 Experiments on the generation of internal waves in a stratified fluid. *AIAA J.* **23**, 693–700.
- HASSID, S. 1980 Collapse of turbulent wakes in stably stratified media. *J. Hydromantics* **14**, 25–32.
- KÄLLÉN, E., JOHANSSON, Å. & LUNDBERG, P. 1984 Vertical wave propagation in a stratified fluid and surface signatures from internal waves (in Swedish). *FOA (Swedish National Research Institute) Rep. C 205556-E1 (D9)*, 44 pp.
- KULLENBERG, G. 1977 Entrainment velocity in natural stratified vertical shearflow. *Estuar. Coast. Mar. Sci.* **5**, 329–338.
- LANDAU, L. D. & LIFSHITZ, E. M. 1959 *Fluid Mechanics*. Pergamon. 536 pp.
- LARSSON, A. M. & RODHE, J. 1979 Hydrographical and chemical observations in the Skagerak 1975–1977. *Department of Oceanography, University of Göteborg Rep.* **29**.
- LIN, J.-T. & PAO, Y.-H. 1979 Wakes in stratified fluids. *Ann. Rev. Fluid. Mech.* **11**, 317–338.
- PHILLIPS, O. M. 1966 *The Dynamics of the Upper Ocean*. Cambridge University Press. 261 pp.
- SHARMAN, R. D. & WURTELE, M. G. 1983 Ship waves and lee waves. *J. Atmos. Sci.* **40**, 396–427.
- SMITH, P. B. 1980 Linear theory of stratified hydrostatic flow past an isolated mountain. *Tellus* **32**, 348–364.